Human Body Model Muscle Activation Influence on Crash Response

Jonas Östh, Emma Larsson, Lotta Jakobsson

Abstract Whole-Sequence simulations consisting of a pre-crash manoeuvre and a crash scenario were carried out to investigate the effect of muscle activation on Human Body Model (HBM) kinematics and injury predictions during crash. A full factorial combination of two pre-crash manoeuvres (Braking and Left Turn), three crash scenarios (two frontal impacts and one Far-Side impact), and four muscle activation strategies (controllers *Off*, *Active*, *Hold* at a constant control signal and with a *Startle* response) were run. It was found that for the frontal impacts, the muscle activation did not have any considerable effect on the kinematic response, however HBM injury predictions were affected in the higher acceleration frontal impact. For the Far-Side impact, there was a moderate effect on kinematics in the form of reduced peak inboard head excursion with active muscles. The recommendation from the study is that muscle activations should also be included in the crash-phase of Whole-Sequence simulations to enable HBM simulation to better represent live occupants. However, as the postural control algorithm appears to give high muscle activations during the crash-phase, a strategy to hold the muscle activations constant during the crash is recommended for now.

Keywords Human Body Model, Finite Element, Active Muscle, Postural Control, Far-Side Impact

I. INTRODUCTION

To date, several Finite Element (FE) Human Body Models (HBMs) for occupant restraint evaluation in vehicle crash simulations have been developed. They are primarily used for research and concept studies, but increasingly are also used for product development in the automotive industry. There are two major occupant HBM families that are commercially available: the Global Human Body Model Consortium (GHBMC) 5th female, 50th male and 95th percentile male detailed occupant models [1–3] and simplified occupant models [4]; and the THUMS v4 5th female, 50th male and 95th percentile models [5]. In addition to these models, the 50th male SAFER HBM [6] is being continuously developed, initially based on the THUMS v3 but as of the current version, most parts have been replaced or updated [6–7].

For impact biomechanics research, the main way to assess injurious loading and find human tolerance limits is to conduct impact tests with Postmortem Human Subjects (PMHS) [8]. Data from PMHS tests are also used extensively to validate HBM crash responses [1–2, 6]. In real-life, however, car occupants tend to be alive, which is why additional modelling of human postural and reflexive muscle responses has been added to HBMs. For the SAFER HBM, the feedback postural control method was used initially for the upper extremity to show proof-of-concept in an FE HBM [9], and has been added to the trunk and neck for simulation of longitudinal kinematics [10], and for omni-directional planar kinematics using spatial tuning patterns recorded from volunteers in perturbation tests [11]. Several attempts to add active muscle control to the THUMS family of HBMs have been made. Some studies used experimentally recorded muscle activations from volunteer Electromyogram (EMG) signals for the lower [12] and the upper extremities [13], others used a reinforcement learning model with a simplified learning model [14], and, for the THUMS v5, and onward feedback postural control [15]. More recently, feedback postural muscle control has been added to the GHBMC family of models, both the simplified 50th male model [16] and the detailed cervical spine [17]. Several other attempts to add active muscle control to HBMs have been made as well, for various versions of the THUMS v3 [18–20] and for the Multibody (MB) Madymo HBM, which was the first whole-body HBM with feedback postural control [21–22].

HBMs with feedback postural muscle control, i.e. Active HBMs, have typically been developed for modelling

J. Östh, PhD, (e-mail: jonas.osth@volvocars.com, tel: +46 728 88 91 72), is a Safety Analysis CAE Engineer and L. Jakobsson, PhD, is a Senior Technical Leader at the Volvo Cars Safety Centre, Gothenburg, Sweden. E. Larsson is a PhD Student, J. Östh an Adjunct Associate Professor and L. Jakobsson an Adjunct Professor at Chalmers University of Technology, Sweden. All authors are associated with SAFER – Vehicle and Traffic Safety Centre at Chalmers in Sweden.

the occupant response in pre-crash events, such as evasive braking [10, 23–24] or steering manoeuvres [25] in combination with pre-crash activated restraints. For studies aimed at the impact, or crash-phase, the effect of muscle activation has also been investigated, but then primarily using pre-defined muscle activation patterns, either from volunteer EMG measurements or through hypotheses about the muscle activations. For instance, it has been shown that neck muscle activation can reduce the load on the cervical capsular ligaments to below the injury threshold [26] and that neck muscles and muscle activation increases the ligamentous cervical spine tolerance from 1.8 kN to 3.1–3.7 kN [27]. Some authors have studied the effect of muscle bracing activations in lower extremity impacts, showing that muscle bracing may give an increase in the Revised Tibia Index (RTI) value from 0.5 to 1.25 for pedal impacts [12], that lower extremity muscle bracing may change bone stress to injury-inducing levels [28], that the likelihood of femoral shaft fracture in knee impacts could be increased by 20–40 % [29–30] with lower extremity muscles tensed to levels gathered from an inverse dynamics musculoskeletal model, and that tensed lower extremity muscle can increase injury risk in frontal impacts with a knee airbag [31]. Upper extremity muscle activation has been shown to increase the stiffness of the extremities in impact [13], and that bracing with the arms can reduce belt loading in crash [32]. The effect of pre-determined muscle activations on in-crash response has also been studied for pedestrian HBMs impacted by cars. Neck muscle activation did not have any major effect on brain strain in such simulations [33], but changes in initial pedestrian position prior to impact [34] could be important. Lower extremity muscle activation was concluded to have the potential to reduce the risk of injury to the knee ligaments, the ribs and the neck in pedestrian impact simulations [35].

Some studies have utilized the postural feedback control developed to provide human-like reactions in the pre-crash phase also in the crash-phase. For instance, an Active HBM with feedback control but low initial co-contractions (relaxed) and an Active HBM with initial co-contracted (braced) muscles were simulated in Whole-Sequence frontal impacts combined with pre-crash braking and reversible pre-tensioned restraints, and it was reported that the muscle activation could have as big an effect on forward displacements as the reversible pre-tensioned belt [36]. Active repositioning from a reclined posture prior to impact was studied with the SAFER HBM, and it was concluded that while repositioning helps regain a nominal initial position, the pelvis angle was not restored to the due flexibility of the spine in the HBM [37], and that the active muscles have the potential to influence the HBM injury predictions from the impact. Far-side lateral impact in a simplified sled setup was studied with another Active HBM [38]. The authors hypothesized and simulated several potential muscle activation strategies. It was recommended to either remove muscle activations for simulation of the crash-phase or to keep them constant at the levels found at the end of the pre-crash phase.

To understand human muscle responses in the crash-phase requires testing of volunteers, which is challenging to conduct. However, several studies with volunteers at loading levels approaching those in the crash-phase are available in the literature – for instance, frontal impacts [39–43] ranging from 2.5 g to 24 g, and rear-end impacts [44–47]. Several of these studies included and analysed the EMG of multiple muscles. EMG is an electrical measurement of the action potential present when the muscle fibre is activated, and through normalization with Maximum Voluntary Contractions (MVCs) prior to testing it is possible to quantify to which extent the measured muscle or muscles were activated, the timing and pattern of muscle activation during the crash event. These studies have shown that considerable restraint forces can be generated through the lower extremities if these are activated before crash by an instruction to brace, i.e. to co-contract and press with the legs, prior to impact [41]. For tests without pre-crash bracing muscle activation there was found to be a reflexive muscle activation response, but the authors concluded that this muscle reflex was too slow to affect the outcome of the crash, as they also measured and reported an electromechanical delay of 80–150 ms from start of the EMG signal until force was recorded at the force transducers. A startle response, which is likely to occur in several impact configurations, has been reported in rear-impacts [44, 46] and even through reversible belt pre-tension [48]. It is a centrally generated reflex, present in most mammals, that can be evoked by sudden visual, acoustic, or somatosensory stimuli [49]. Startle is characterized by a bilateral response that includes closing of the eyes, extension of the neck, elevation of the shoulders and extension of the lumbar back. In volunteer testing with EMG measurements, it is detected as a short, bilateral, simultaneous activation burst of all muscles, which can reach higher than 100 % of the MVC values recorded [44, 48]. Furthermore, once in the crash-phase, the occupant will be displaced, which causes forced lengthening of muscles that is likely to elicit a stretch reflex response of the muscle [50]. For cervical muscles, the stretch reflex time was reported to be in the order of 62–90 ms, with lower values for females and younger subjects compared with males and older subjects, respectively. Reflex reaction

times for the muscles in the human body are shorter the closer to the central nervous system the muscle is situated, which is why for the cervical muscles reaction times as short as 13 ms from head acceleration onset have been reported [45]. Lastly, volunteers in a simulator study subject to a simulated frontal impact with a truck were reported to extend their arms against the steering wheel and brace rearward into the seat, or to steer to try to avoid the accident [51]. This review of volunteer muscle responses in crash scenarios indicates a number of possible human reactions to a crash. They include a startle response that could be modelled as a short muscle activation burst, a stretch reflex response that could be modelled in an Active HBM by keeping the muscle control activated in the crash as the feedback postural control algorithms will react similar to a stretch reflex (in some cases they are actually modelled as stretch reflexes [38, 52]), or a bracing response that would consist of co-contraction of the muscles prior to the impact.

The aim of this study was to evaluate the effect of different muscle activation strategies on the HBM kinematics and injury predictions in Whole-Sequence crash simulations, consisting of both a pre-crash manoeuvre and a crash scenario.

II. METHODS

Simulations were made using LS-DYNA MPP R9.3.1 (SVN 141945, ANSYS/LST, Livermore, CA) with the SAFER HBM v10 [6, 7], which is a 50th percentile male occupant model of 175 cm stature with a mass of 77 kg, including use of the postural feedback muscle control system.

SAFER HBM Muscle Control System

The SAFER HBM utilizes an Angular Position Feedback (APF) postural control scheme, for which the control signal, *u(t)*, is a function of the magnitude, the rate of change and the integrated error over time for the angle between a body segment vector, $\boldsymbol{v}_{t-\tau_d}$, and a reference vector, $\boldsymbol{v}_{ref}$: Equations (1) and (2). The controller gains, k_p, k_i and k_d, have been tuned with respect to volunteer responses in braking sled tests and validated for passenger and driver responses in braking interventions [10, 25]:

$$e(t) = \theta_{t-\tau_d} = cos^{-1}\left(\frac{\boldsymbol{v}_{t-\tau_d} \cdot \boldsymbol{v}_{ref}}{|\boldsymbol{v}_{t-\tau_d} \cdot \boldsymbol{v}_{ref}|}\right) \quad (1)$$

$$u(t) = k_p e(t) + k_i \int_0^t e(\tau)d\tau + k_d \frac{d}{dt}(e(t)) \quad (2)$$

Two controllers were used for the axial skeleton, one for a vector from T1 to the head centre of gravity, and one for the trunk, for a vector from sacrum to the T10 vertebra (see Fig. 1). The calculation of the error signal, Equation (1), accounts for a delay, τ_d, to represent the time needed for neural propagation and the time needed to bridge the synapses of the sensorimotor control pathways. The control signals, *u(t)*, Equation (2), were directed to muscle activation functions, Equations (3) and (4), consisting of two coupled first order filters representing the dynamics from muscle stimulation to force generation. The intermediate neural excitation signal, $N_e(t)$, in this model should be representative of a lightly filtered EMG signal [53] and the muscle activation $N_a(t)$ proportional to the force generated by the muscle so that a *Na* of 1 is equal to 100% MVC contraction. The timing difference between the N_e and N_a signals is thus the electromechanical delay [41, 50] from EMG signal to muscle force generation.

$$T_{ne}\frac{dN_e}{dt} = u(t) - N_e(t) \quad (3)$$

$$T_{na}\frac{dN_a}{dt} = N_e(t) - N_a(t) \quad (4)$$

To enable omnidirectional control the control signal, *u(t),* is passed through a spatial tuning function [11, 25] which activates muscles based on the direction in which the error signal is generated (Fig. 1). Co-contraction of antagonistic muscles was included in the modelling though antagonist activity in spatial tuning patterns. The spatial tuning groups of the SAFER HBM are presented in Fig. A1–A2 in the Appendix. Furthermore, a baseline activity was added to the signal, to represent the activity in the muscles during quiet sitting.

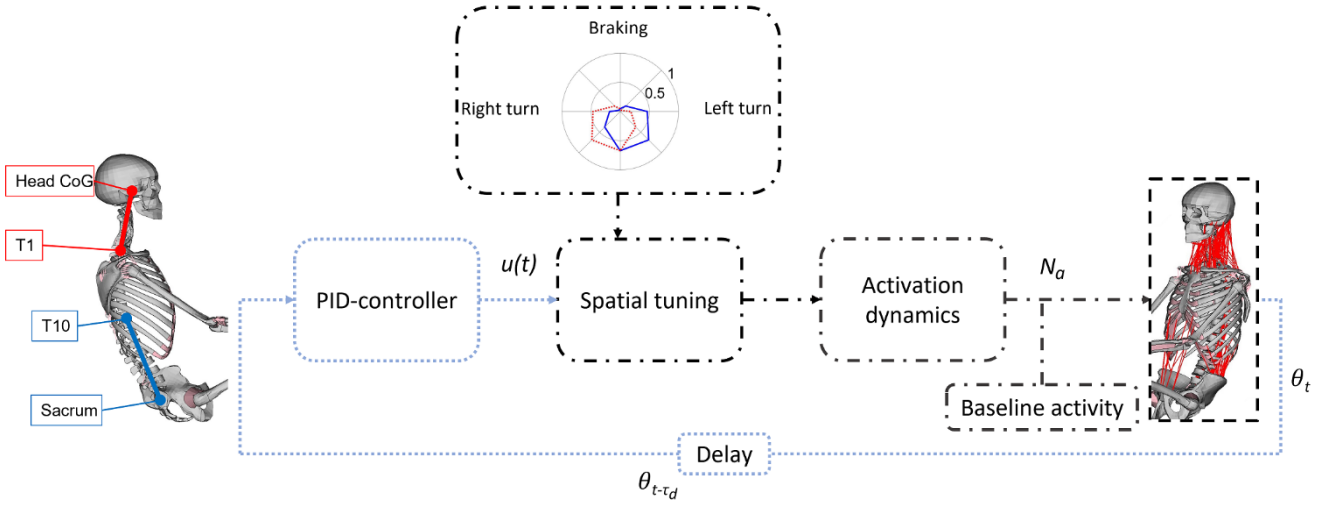

Fig. 1. Schematic representation of the SAFER HBM's APF postural control. Blue dotted lines represent signals common for the whole control system, black dash-dotted lines represent signals on muscle-specific level.

Whole-Sequence Crash Simulations

Five Whole-Sequence crashes were created through a combination of two pre-crash manoeuvres and three crash scenarios (Table I). The pre-crash manoeuvres simulated were a Braking and a turning (Left Turn) event. The Braking had a peak acceleration amplitude of 11 m/s^2 and a rise time of 200 ms from 150 ms into the event, and the Left Turn was simulated as the 6m/s^2 lateral acceleration from the initial part of a double lane change manoeuvre [54]. The three crash scenarios were: a 56 km/h Full-Frontal Rigid Barrier (FFRB) impact pulse; a Mobile Progressive Deformable Barrier (MPDB) impact pulse from a simulation of a 1400 kg trolley impacting a large size SUV with 50 % overlap with both vehicles at 50 km/h; and a Far-Side impact at the front left corner of the struck vehicle, travelling at 31 km/h, and being hit by a car with a velocity of 52 km/h [55].

TABLE I.
WHOLE-SEQUENCE CRASH SIMULATION MATRIX.

Sequence	Initialization (ms)	Pre-Crash Manoeuvre	Pre-Crash Duration (ms)	Crash Scenario	Crash Duration (ms)	Total Simulation Time (ms)
1	300	Braking	500	FFRB	120	920
2	300	Braking	500	MPDB	120	920
3	300	Braking	500	Far-Side	300	1100
4	300	Left Turn	850	MPDB	120	1270
5	300	Left Turn	850	Far-Side	300	1450

All Whole-Sequence crashes were simulated in a FE rigid car body occupant compartment simulation model, with the SAFER HBM positioned in the passenger seat, in an upright posture with the arms and hands to the side of the legs (Fig. 2). The seat was in its lowest position, and at mid fore-aft travel length, with a seat-back angle of 25°. A three-point seat belt with a pyro-technical pretensioner and a single stage load-limiter was used in all simulations. A passenger airbag deploying upward from the instrument panel was activated in the frontal crash simulations.

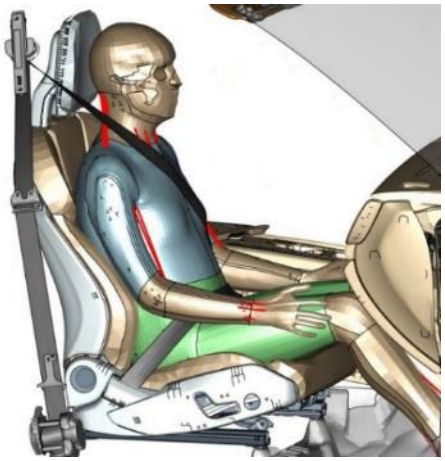

Fig. 2. Initial position of the SAFER HBM in the occupant compartment sled model used for the Whole-Sequence crash simulations.

Muscle Activation Strategies

The pre-crash manoeuvres were all simulated with the SAFER HBM APF postural control active, while all crash scenarios were simulated using four muscle activation strategies, identified from the review of volunteer studies, giving a total of 20 Whole-Sequence simulations. The first muscle activation strategy was to turn *Off* the muscle control algorithm at the start of the crash-phase, giving a baseline HBM response without muscle activation during the crash. The second strategy was to keep the muscle control algorithm *Active* during the crash-phase, thereby extrapolating the stretch reflexes and postural reflex responses which the controller generates as a response to postural change, and which has been validated in the pre-crash phase [10, 25]. The third strategy was to *Hold*, which was to freeze the muscle control signal at the end of the pre-crash phase and thereby keep the muscle activations generated during the pre-crash phase but not updating the control signal during crash. The fourth and final strategy was to complement the Hold strategy with constant control signal with a *Startle* response, modelled as a triangular impulse (see Fig. A8 in the Appendix) in the control signal *u(t)* to all muscles, with an amplitude of 100% and a duration of 100 ms, starting 50 ms into the crash event, at the shorter end of the time interval for startle responses reported experimentally [44–46].

III. RESULTS

The Whole-Sequence simulations were run on 120–140 CPU with a total simulation time of 80–226 h. The longest duration was for the Left Turn followed by a Far-Side crash, while the shortest duration was for the Braking and FFRB or MPDB crash simulations. All simulations reached the full simulation time (Normal Termination).

Pre-Crash Kinematics

The two pre-crash manoeuvres gave different initial occupant positions at the start of the crash-phase (Fig. 3). The Braking manoeuvre gave a T1 vertebra position that was 176 mm forward of the initial position. For the Left Turn the T1 was 70 mm forward and 96 mm outboard. For the head, the position was 245 mm forward after the Braking and 180 mm more outboard after the Left Turn.

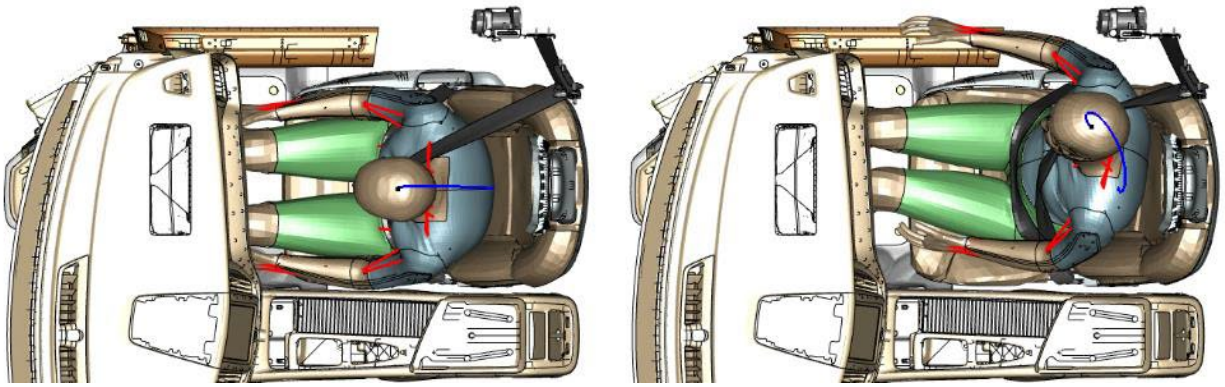

Fig. 3. Initial position at the start of the crash scenario after the pre-crash Braking manoeuvre (left) and the Left Turn manoeuvre (right). The blue line shows the head centre of gravity trajectory during the pre-crash phase.

Pre-Crash Muscle Activations

The pre-crash manoeuvres lead to muscle activation control signals *u(t)*, Equation (2), for the cervical and lumbar controller, which started to be generated from around 100 ms into the pre-crash manoeuvres (Fig. 4). For the Left Turn manoeuvre the control signal was stabilized at the end of the pre-crash phase and the muscle activations were therefore relatively stable at the start of the crash scenarios.

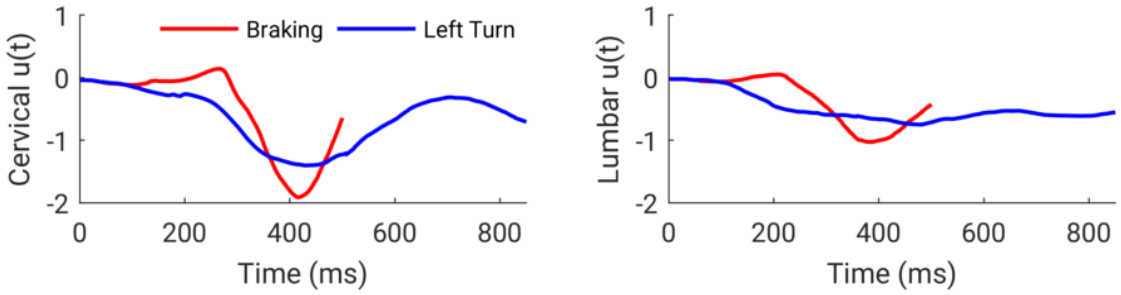

Fig. 4. Control signal histories for the pre-crash manoeuvres.

The change from positive to negative for both the cervical and the lumbar control signal from around 200 ms to 400 ms (Fig. 4) lead to an increase in extensor muscle activation, starting at 300 ms (Fig. 5). The highest activations were found for the cervical extensor muscle Splenius Capitis (SCap) and the Lumbar Multifidus (LMF) extensors. For the Braking manoeuvre the activations were symmetrical on the left and right side.

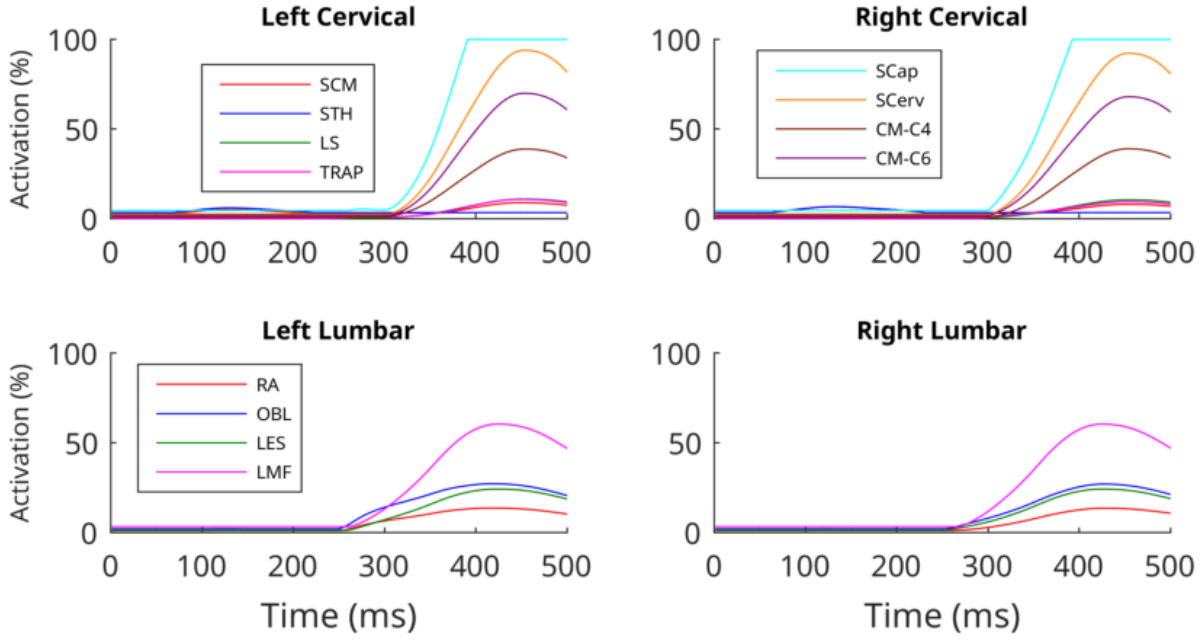

Fig. 5. Time histories of the SAFER HBM muscle tuning group activation levels during the Braking pre-crash manoeuvre. See Fig. A1–A2 in the Appendix for an illustration of the muscle spatial tuning group abbreviations.

For the Left Turn manoeuvre (Fig. 6) the Sternocleidomastoid (SCM) and Sternohyoid (STH) muscles in the cervical spine and the abdominal obliques (OBL) of the lumbar controller were the most active, and more so on the left side to counteract the outboard motion of the occupant due to the lateral acceleration.

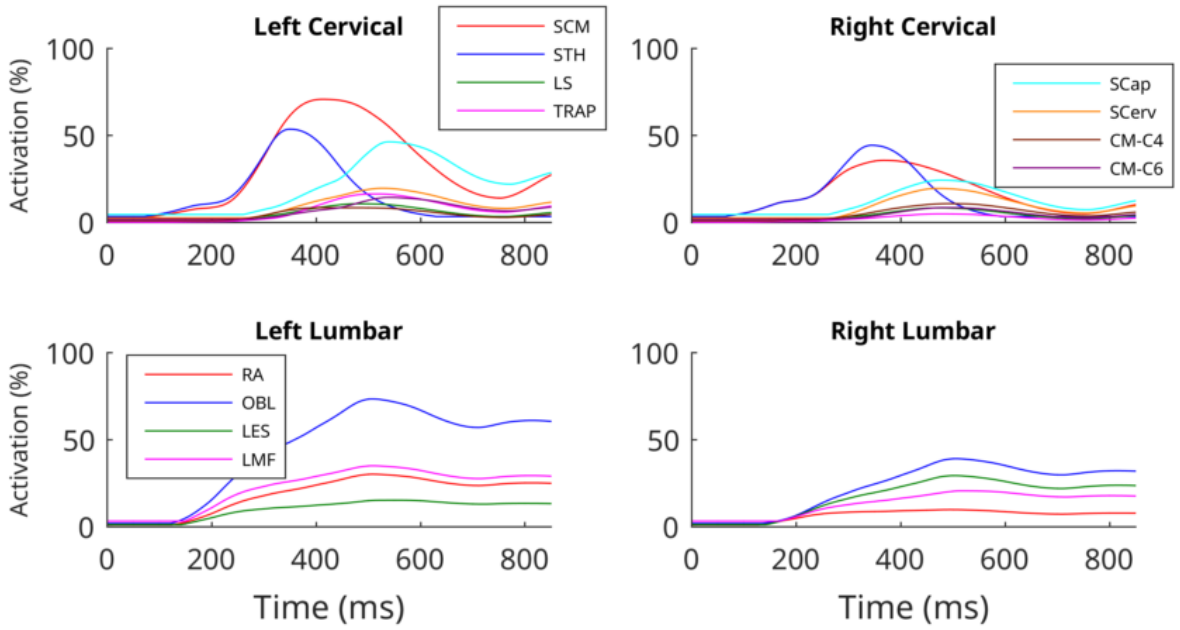

Fig. 6. Time histories of the SAFER HBM muscle tuning group activation levels during the Left Turn pre-crash manoeuvre. Fig. A1–A2 in the Appendix for an illustration of the muscle spatial tuning group abbreviations.

Crash Kinematics

For the frontal impact Whole-Sequence crash simulations (Fig. 7) the peak forward displacements of the occupant were similar regardless of the muscle activation strategy employed. One difference in crash kinematics was noted for the simulations with the strategy to turn the muscle controllers *Off,* for which the head followed a trajectory that was 10–20 mm above the active models, and the T1 vertebra 7–8 mm above.

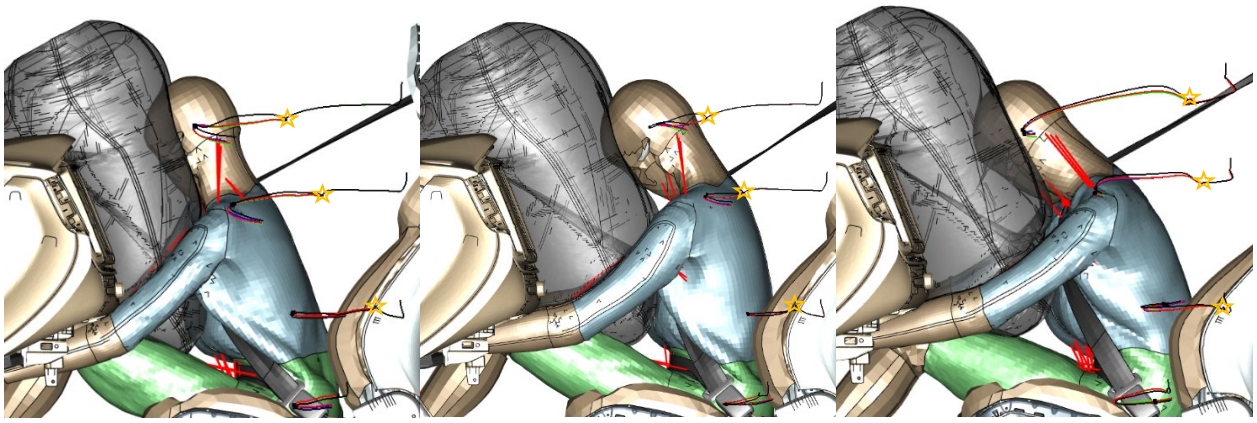

Fig. 7. Occupant trajectories for the head centre of gravity, T1 vertebra, T12 vertebra, and Sacrum in the Whole-Sequence simulations (pre-crash and crash). The stars indicate the transition from pre-crash to crash. The snapshots were taken of the HBM in the most forward position in the simulation with the muscle controller turned *Off* during the crash-phase (black trajectories), while the *Active* strategy was plotted with red trajectories, the *Hold* with blue and the *Startle* with green. *Left*: Sequence 1, Braking followed by FFRB. *Middle*: Sequence 2, Braking followed by MPDB. *Right*: Sequence 4, Left Turn followed by MPDB.

For the Far-Side impacts (Fig. 8) there were more variations of the head trajectory than for the frontal impacts, while the T1 trajectory did not vary as much between activation strategies during crash. The peak inboard lateral displacement of the head centre of gravity was largest with the controller turned *Off*, 380 mm and 383 mm, for Far-Side impact after Braking (Sequence 3) and Left Turn (Sequence 5), while it was smallest with the *Startle* muscle activation strategy, 355 mm and 342 mm, respectively. During the rebound phase, there was more influence of the muscle activations strategies, with the Startle strategy giving a head location some 100–150 mm more forward than the *Hold* or *Off* strategies, at the end of the simulation.

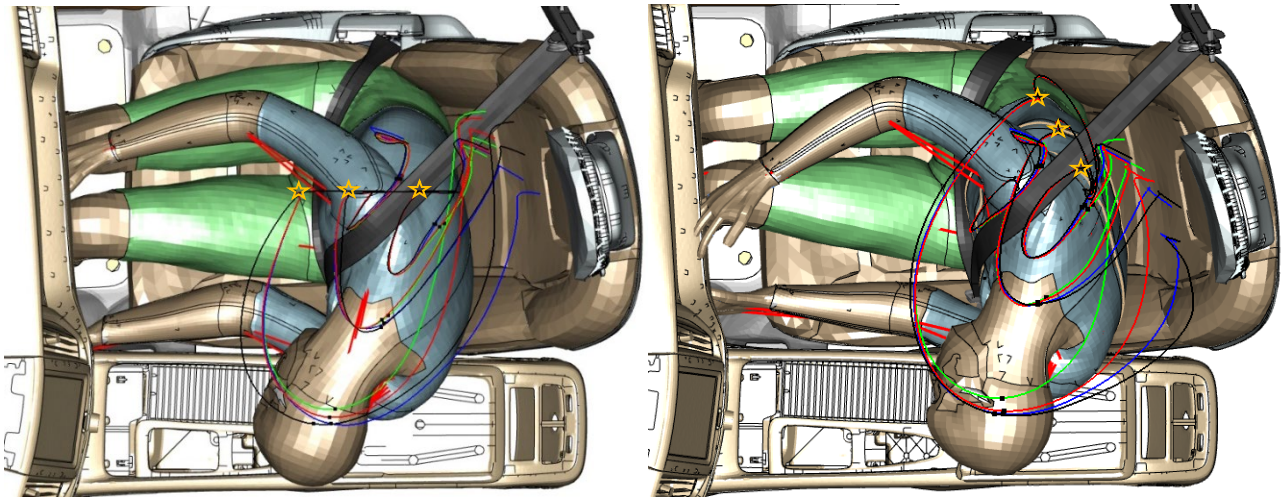

Fig. 8. Occupant trajectories for the head centre of gravity, T1 vertebra, T12 vertebra, and Sacrum in the Whole-Sequence simulations (pre-crash and crash). The stars indicate the transition from pre-crash to crash. The snapshots were taken of the HBM in the most forward position in the simulation with the muscle controller turned *Off* during the crash-phase (black trajectories), while the *Active* strategy was plotted with red trajectories, the *Hold* with blue and the *Startle* with green. *Left*: Sequence 3, Braking followed by Far-Side impact. *Right*: Sequence 5, Left Turn followed by Far-Side impact.

Crash Muscle Activations

The control signal amplitudes were considerably higher during the crash-phase for the simulations with the *Active* muscle control strategy (Fig. 9) than during the pre-crash manoeuvres (Fig. 4). The control signals were highest for the Far-Side impact, with peak values of −8 and −6.5 for the cervical and lumbar controller, respectively, compared to −1.45 and −0.75 for the Left Turn pre-crash manoeuvre (Fig. 4). For the FFRB impact, peak control signal values were −5.0 and −6.4 for the cervical and lumbar controllers, respectively. For comparison, the corresponding values during the Braking manoeuvre were −2.0 and −1.0 (Fig. 4).

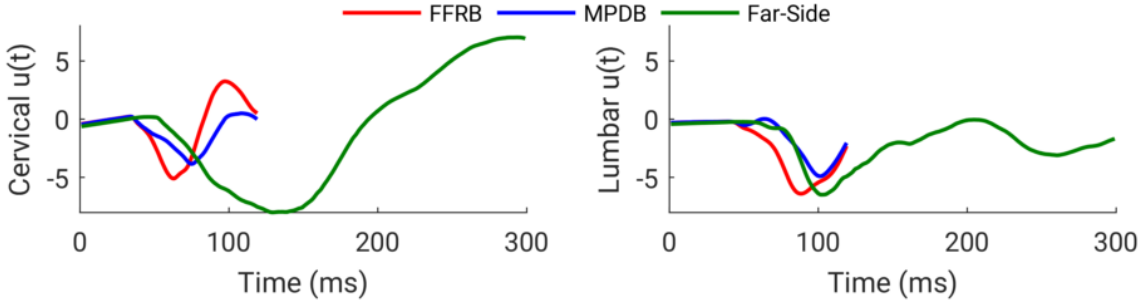

Fig. 9. Cervical and lumbar control signal histories for the impact scenarios with the *Active* muscle control strategy, after the Braking pre-crash manoeuvre (Sequence 1–3).

As a result of the higher control signals during the crash scenarios, several muscle activations were reaching 100% activation during the later stage of the frontal impacts (Fig. 10). After the pre-crash braking manoeuvre, the cervical extensor muscles Splenius Capitis (SCap) and Splenius Cervicis (SCerv) had high activations already at the start of the crash and the activations were slowly decreasing until the rapid change of posture due to the crash pulse led to increased activation, which was also seen for the lumbar extensors, such as the Lumbar Multifidus (LMF).

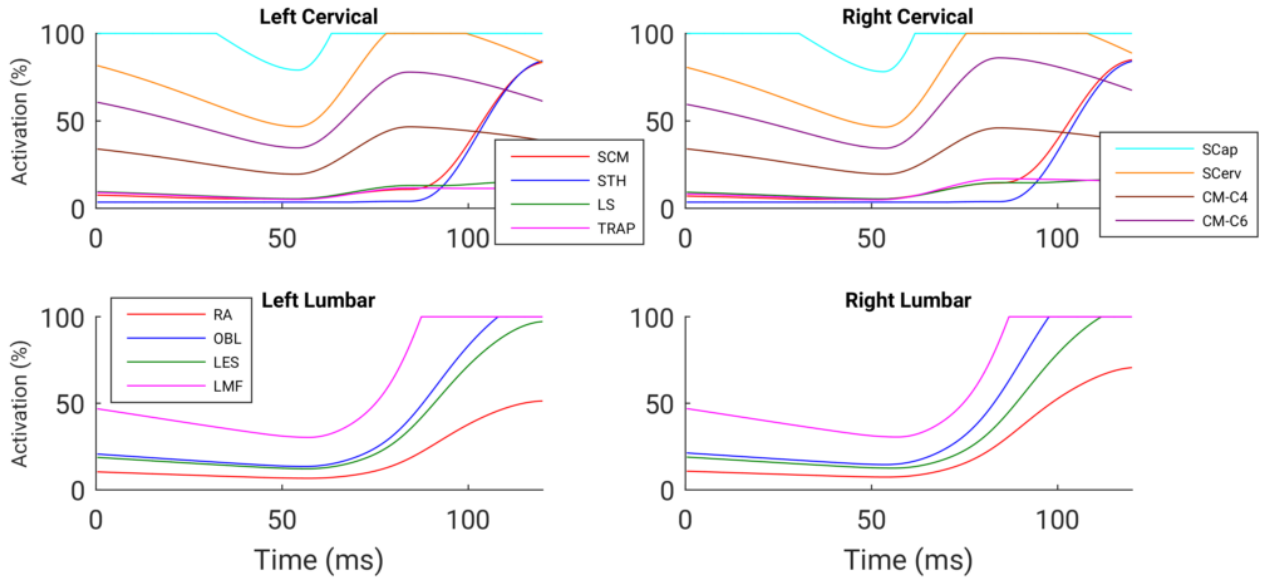

Fig. 10. Time histories of the SAFER HBM muscle tuning group activation levels during the FFRB crash after the pre-crash Braking manoeuvre with the *Active* muscle control strategy (Sequence 1). See Fig. A1–A2 in the Appendix for an illustration of the muscle spatial tuning group abbreviations.

The muscle activations in the Far-Side crash after the Left Turn manoeuvre (Sequence 5) were lower at the start of the event (Fig. 11) and more complex during the crash. First SCap cervical extensor on the left side responded with increased activation at 70 ms, due to the HBM hanging in the belt outboard and first moving forward during the crash-phase. Following the activation of the left side cervical extensors, the right-side extensors were also activated, starting with SCap at 95 ms, due to this forward movement. At around 150 ms the right-side Sternocleidomastoid (SCM) started activating in response to the HBM now moving inboards. The lumbar extensors activated bilaterally from around 90 ms, and after 200 ms there was more activation in the right-side lumbar muscles in response to the inboard occupant movement during the Far-Side crash.

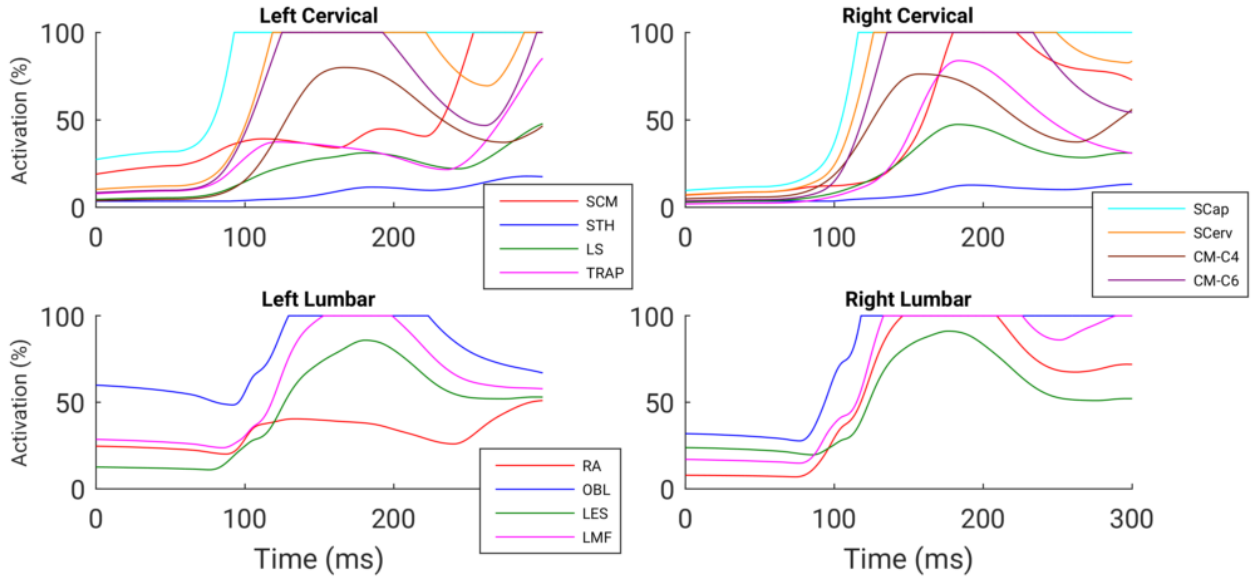

Fig. 11. Time histories of the SAFER HBM muscle tuning group activation levels during the Far-Side crash after the pre-crash Left Turn manoeuvre with the *Active* muscle control strategy (Sequence 5). See Fig. A1–A2 in the Appendix for an illustration of the muscle spatial tuning group abbreviations.

As a result of the higher magnitude control signals during the crash scenarios, several muscles reached 100% activation during the crash-phase (Table II). In particular, the cervical extensors SCap and SCerv and the lumbar LMF extensors, which were saturated in almost all *Active* muscle strategy crash simulations. The SCM, which is primarily a cervical flexor activated during lateral motions of the head and neck, reached 100 % activation in the Far-Side impact simulations, but not in the frontal impact ones. Both Levator Scapulae (LS) and Trapezius (TRAP), which were attenuated by the spatial tuning patterns, have moderate to low activations, with the exception of

the right TRAP in Far-Side impact after Braking. Additional time histories of muscle activations for Sequence 2, 3 and 4 and with the *Off*, *Hold* and *Startle* muscle activation strategies are included in Fig. A4–A9 in the Appendix.

TABLE II

MUSCLE SPATIAL TUNING GROUP PEAK ACTIVATIONS DURING THE CRASH-PHASE FOR SIMULATIONS WITH THE CONTROLLER ALGORITHM ACTIVE DURING THE CRASH SIMULATIONS.

Pre-Crash Maneuver	Crash Scenario	SCM		STH		LS		TRAP		SCap		SCerv		CMC4		CMC6		RA		OBL		LES		LMF	
		L	R	L	R	L	R	L	R	L	R	L	R	L	R	L	R	L	R	L	R	L	R	L	R
Braking	FFRB	83	85	84	84	15	16	12	17	100	100	100	100	47	46	78	86	51	71	100	100	97	100	100	100
Braking	MPDB	14	15	10	9	11	12	11	15	100	100	93	95	39	39	69	72	30	59	77	100	61	74	100	100
Braking	Far-Side	100	100	37	24	42	53	59	100	100	100	100	100	84	77	100	100	44	100	100	100	100	100	100	100
Left Turn	MPDB	71	36	54	44	27	16	50	14	100	100	100	80	43	48	100	56	73	22	100	78	70	53	100	93
Left Turn	Far-Side	100	100	53	44	48	47	85	84	100	100	100	100	80	76	100	100	51	100	100	100	86	91	100	100

Injury Predictions

For both the MPDB and the Far-Side impacts, the HBM had low injury criteria and injury risk levels regardless of the pre-crash manoeuvre (Table III). For instance, the highest Head Injury Criterion (HIC_{15}) value for any of these simulations was 83 and the risk for two or more rib fractures (NFR) was zero. However, for the Far-Side impact with the muscle controller turned *Off* after pre-crash braking, the predicted risk for AIS1+ Concussion (CC) [57] was 44 %. This resulted from a peak in brain Maximum Principal Strain (MPS) as the head reached the peak lateral excursion (Fig. 8) and the neck bent over considerably, but without any head impact to the vehicle interior.

For the FFRB crash scenario, which has a higher peak acceleration and delta V, the HBM had a HIC_{15} of 199, a predicted AIS 1+ CC risk of 45 %, an N_{ij} of 0.22 and a 32 % risk NFR2+ for a 45 Year Old (YO) [58], all for the baseline simulation with the muscle controller turned *Off*.

For several evaluated injury criteria, there was a trend that keeping the muscle controller active reduced the HBM's injury criteria and predicted injury risk levels. For the FFRB impact, lower head and neck injury criteria were seen, except for a negligible higher peak neck flexion moment (My+). For the NFR2+ rib fracture risk, there was a decrease from 32 % with 19–22 %, based on peak rib strain reductions of 0.24–0.9 % (from 1.9 % to 2.4 %) for the left side (inboard) ribs at ribs 5–9 (Fig. A12 in the Appendix).

However, for the peak L5 lumbar spine compressive load (L5 Fz−) higher values in several of the simulations with the muscle controller active were seen, by up to 0.92 kN higher peak load for the Far-Side crash after Left Turn with the muscle controller *Active* (Fig. A11 in the Appendix).

TABLE III

EFFECT OF MUSCLE ACTIVATION STRATEGIES ON HBM INJURY CRITERIA AND RISK LEVELS. THE SIMULATION WITH THE MUSCLE ACTIVATION TURNED OFF (OFF) PRESENTS THE BASELINE VALUE, AND VALUES FOR THE SIMULATIONS WITH THE MUSCLE CONTROLLER *ACTIVE*, WITH A CONSTANT CONTROL SIGNAL (*HOLD*) AND WITH A *STARTLE* RESPONSE ARE CALCULATED RELATIVE TO THE BASELINE VALUE. LOWER MAGNITUDE VALUES THAN THE BASELINE ARE COLOR CODED WITH GREEN AND HIGHER WITH RED. N/A = NOT APPLICABLE.

Pre-Crash Maneuver		Braking												Left Turn							
Crash Scenario		FFRB				MPDB				Far-Side				MPDB				Far-Side			
Muscle Strategy	Unit	Off	Active	Hold	Startle	Off	Active	Hold	Startle	Off	Active	Hold	Startle	Off	Active	Hold	Startle	Off	Active	Hold	Startle
HIC15	(-)	199	-22	-31	-23	83	-27	-33	-30	18	-7	-10	-8	65	-5	-4	0	15	1	3	0
DAMAGE	(-)	0.33	-0.11	-0.11	-0.11	0.19	0.02	0.01	0.01	0.21	-0.07	-0.07	-0.07	0.28	-0.07	-0.06	-0.07	0.22	-0.05	-0.05	-0.03
MPS	(-)	0.29	-0.04	-0.03	-0.03	0.19	0.01	-0.01	0.00	0.29	-0.14	-0.13	-0.19	0.22	-0.06	-0.05	-0.05	0.17	0.01	0.03	-0.02
CC AIS1+	(%)	45	-9	-8	-7	24	2	-2	0	44	-28	-26	-33	29	-10	-9	-9	21	2	4	-3
Neck Fz+	(kN)	1.07	-0.56	-0.58	-0.59	0.62	-0.26	-0.33	-0.31	0.85	-0.21	-0.27	-0.14	0.64	-0.02	-0.02	-0.01	0.71	0.05	0.11	0.04
Neck Fz-	(kN)	-0.84	0.52	0.47	0.52	-0.84	0.68	0.68	0.69	-0.86	0.70	0.67	0.70	-0.45	0.09	0.08	0.10	-0.38	0.10	0.12	0.12
Neck My+	(Nm)	23.7	0.9	1.1	1.9	22.8	3.1	3.2	2.9	22.3	1.7	3.0	3.0	15.8	-5.2	-5.5	-6.5	16.8	14.8	-5.8	-6.8
Neck My-	(Nm)	-10.6	9.9	9.9	7.8	-6.1	5.4	5.4	1.6	-4.8	-1.0	1.2	2.5	-5.7	4.6	4.6	1.0	-17.0	2.8	-0.9	3.4
Nij	(-)	0.22	-0.10	-0.10	-0.09	0.19	-0.08	-0.09	-0.09	N/A	N/A	N/A	N/A	0.14	-0.02	-0.02	-0.02	N/A	N/A	N/A	N/A
NFR2+ 45 YO	(%)	32	-22	-19	-22	0	0	0	0	0	0	0	0	0	0	0	0	0	0	0	0
L5 Fz-	(kN)	-1.51	-0.78	-0.21	-0.55	-1.04	-0.41	-0.44	-0.47	-1.10	-0.86	0.00	-0.49	-1.13	-0.72	-0.77	-0.83	-0.98	-0.92	-0.44	-0.57
L5 My+	(Nm)	55.6	-0.1	-3.3	-1.5	35.7	0.1	0.4	1.4	20.9	1.3	1.2	1.3	39.5	-0.4	0.1	0.4	23.2	1.4	1.6	1.8

IV. DISCUSSION

Whole-Sequence crash simulations were carried out to investigate the effect of muscle activation on HBM crash kinematics and injury predictions. In total, 20 simulations were made, a full factorial combination of two pre-crash manoeuvres (Braking and Left Turn), three crash scenarios (FFRB, MPDB, Far-Side) and four muscle activation strategies: controllers *Off*, *Active*, *Hold* at a constant control signal, and with a *Startle* response.

The SAFER HBM has been validated for front crash with focus on the injury prediction of the rib cage [59, 60] and for far-side kinematics [6]. These studies have been made using the model with the muscle control turned *Off*, which is appropriate as the HBM would then behave as a PMHS used in the experimental study against which the HBM was validated to. Activating the muscles, as in this study, is a way to bridge the gap between a model that is PMHS-like, to possible live human occupant responses. In this study, the four simulated muscle activation strategies were selected to allow for evaluation of the effect of human muscle responses on the occupant response in a simulated crash scenario.

The *Active* strategy extrapolates the APF control from modelling muscle activation in response to proprioceptive feedback in the pre-crash phase to the crash-phase. In the Whole-Sequence simulations crash-phase, amplitudes of the control signals were 2.5 and 5.5 times higher for the cervical and lumbar controller, and were 6.4 and 8.7 times larger, during frontal impact compared to braking and Far-Side impact compared to Left Turn, respectively. Resulting peak muscle activations were found to be saturated at 100 % for several muscles during crash (Table II). Maximal and even supramaximal muscle activation has been reported, for instance for cervical muscle during rear-impact [44], but it is likely that the APF control strategy overestimates the muscle response during the crash-phase as it has been tuned for pre-crash displacement amplitudes and rates [10].

The *Startle* strategy was implemented as a triangular activation burst (Fig. A8) starting after an assumed reaction time of 50 ms, in the order of magnitude reported for rear end impacts [44–46]. It leads to a bilateral synchronized burst of muscle activations. Hence, it has some physiological motivation [49]. It can be seen from the muscle activation time history, though, (Fig. A8) that the increase in muscle activation caused by this assumed startle is relatively slow in relation to the crash pulse duration. Peak activations are reached first at the end of the 120 ms crash simulation time for the MPDB crash. This is to some extent in agreement with observations from volunteer crash tests, that the muscle activation can be too slow to affect the primary restraint period [41]. For the Far-Side impact scenario, however, which is longer, there was some influence on peak inboard head displacement, and also for the rebound phase during which the head ended up 100–150 mm more forward at the end of the simulation than for the other activation strategies (Fig. 8).

The *Hold* strategy froze the control signal at the start of the crash-phase. Therefore, the muscle activations were almost constant at the level predicted at the end of the pre-crash phase (Fig. A7) in the Appendix. This strategy does not have a physiological basis, but is straightforward to implement modelling-wise, and acknowledges that muscle activation, if simulated using a validated and biofidelic controller strategy in the pre-crash-phase should be included in a crash simulation as muscle activation changes the outcome of a crash, as shown for the FFRB crash in this study and for several other body parts and impacts in previous work [26–32]. The difference on the controller angles, i.e. the error signals according to Equation (1), between each of the activation strategies were minor (Fig. A3 in the Appendix), but with the controller turned *Off* it can be seen that a larger error is generated.

The influence of the muscle activations on the kinematics in both frontal impacts was minor, and was moderate for the far-side impact. The HBM ends up more or less in the same maximum excursion positions regardless of the muscle control strategy. For the simulated FFRB impact, however, the HBM injury criteria and injury risk predictions were affected. Mostly, the HBM injury criteria were reduced by muscle activations, to an extent that could be of importance for assessing the restraint system's performance. For instance, all muscle activation strategies led to 19–22 % lower risk of NFR2+ for the rib cage. This is an effect of muscle restraint of the torso, which is not effective in stopping the overall motion of the HBM but reduces the load on the rib cage and the strain of the highest loaded ribs on the inboard (left) side (Fig. A12 in the Appendix). This finding is in-line with other studies on the influence of muscle activation on injury prediction showing protective effects, for instance for the cervical spine [26].

For the lumbar spine, an injury assessment reference value of 4.5 kN compressive force [61] for 50% risk of fracture can be used, and relative to this the reported lumbar spine compressive loads in this study are well below the limit. However, for other situations – such as, for instance, a more reclined posture – lumbar loads are likely

to be increased, whereby the additional up to 0.92 kN increase due to muscle activation (Fig. A11 in the Appendix) found in the present work could affect the interpretation of results. This can be compared to similar findings indicating increased leg fracture risk with muscle contraction [29–31]. To summarize – just as in previous work, this study shows that muscle activation in HBM crash simulation can have both possible protective and risk-increasing effects.

The pre-crash manoeuvre simulations resulted in 245 mm forward head displacement due to a 11 m/s^2 braking intervention, which is just on the outer margin of the volunteer mean +1 Standard Deviation (SD) for average male volunteers in a similar amplitude braking [11]. Furthermore, during maximal braking, cervical extensor muscle activations of 17 % (SD 9 %) measured at the C4 level were reported in the same study [11]. The C4 cervical multifidus muscle group (CM-C4) in the HBM is the group that best corresponds to this experimentally evaluated muscle group, and for the HBM higher muscle activations of 39 % were found in the simulations here (Fig. 5). The other cervical extensors in the HBM had even higher activations, indicating that the model uses more of its available strength to maintain the posture than do the volunteers. For the same manoeuvre, average male volunteer lumbar paravertebral muscle activations were reported to be 29 % (SD 23.1 %) [11], while the HBM peak activations were 24 % and 60 % for the Lumbar Erector Spinae (LES) and LMF, respectively.

For the Left Turn pre-crash manoeuvre, the 180 mm outboard head centre of gravity displacement was somewhat higher than for the males exposed to the same lateral acceleration in [54], but within a 1 SD corridor with a peak mean of 150 mm and SD of 65 mm. For the muscles on the opposite side of the movement during the turn, for instance left SCM and the left oblique (OBL) abdominal muscles, peak activations of 71 % and 73 % were found for the HBM. For the males in a volunteer test with the same type of manoeuvre [56], the mean activations of these muscle groups during this part of the event were elevated from the baseline level, but were considerably lower than for the HBM simulations here.

At present, data for validation of HBM in-crash muscle responses are unavailable, hence the levels cannot be verified, therefore the recommendation based on this work is similar to that of Gonzalez-Garcia, et al. [38]: to run HBMs in Whole-Sequence crash simulation with the muscle activation levels frozen from the start of the crash-phase. For the future, the authors encourage work that would enable detailed validation of occupant muscle responses in crash, which we consider necessary to accurately capture the crash response of real, live humans subjected to crash loading.

V. CONCLUSIONS

In this study, Whole-Sequence crash simulations were carried out to investigate the effect of muscle activation on HBM crash kinematics and injury predictions. It was found that for frontal impacts with seat belt and airbag, muscle activation did not have any considerable effect on the kinematic response, but HBM injury predictions were affected in the higher acceleration impact. For a full-frontal rigid barrier impact at 56 km/h, the risk for two or more rib fractures was reduced by 20% while the peak lumbar spine compressive load was up to 0.78 kN higher. For a Far-Side impact, there was a moderate effect on kinematics in the form of peak inboard head excursion. Startle muscle activations reduced the peak inboard head excursions by 25–41 mm, while low baseline injury predictions for the scenario were not affected other than a similar increase in lumbar compressive load due to the muscle contraction. The recommendation from the study is that muscle activations should also be included in the crash-phase of Whole-Sequence simulations, to enable HBM simulation to help better represent live occupants. However, as the postural control algorithm appears to give high muscle activations during the crash-phase, a strategy to hold the muscle activations constant during the crash is recommended for now.

VI. ACKNOWLEDGEMENTS

The authors would like to thank Lara Wehrmeyer, Arturo Pérez Calero, and Pablo Lozano Gil for contributions in setting up the Whole-Sequence crash simulations as part of their MSc Thesis projects at Volvo Cars Safety Centre. This work was carried out at SAFER, Vehicle and Traffic Safety Centre at Chalmers University of Technology, Gothenburg, Sweden, and funded by FFI-Strategic Vehicle Research and Innovation, by Vinnova, the Swedish Energy Agency, the Swedish Transport Administration and the Swedish vehicle industry.

VII. REFERENCES

[1] Davis, M., Koya, B., Schap, J. M., Gayzik, F. S. (2016) Development and Full Body Validation of a 5th Percentile Female Finite Element Model. *Stapp Car Crash Journal,* **60**: pp.509–544.

[2] Davis, M. L., Vavalle, N. A., Gayzik, F. S. (2015) An Evaluation of Mass-Normalization using 50th and 95th Percentile Human Body Finite Element Models in Front Crash. *Proceedings of the IRCOBI Conference*, Lyon, France.

[3] Park, G., Kim, T., *et al.* (2014) Evaluation of the Biofidelity of the Finite Element 50th Percentile Male Human Body Model (GHBMC) under Lateral Shoulder Impact Conditions. *Proceedings of the IRCOBI Conference*, Berlin, Germany.

[4] Schwartz, D., Guleyupoglu, B., Koya, B., Stitzel, J.D., Gayzik, F.S. (2015) Development of a Computationally Efficient Full Human Body Finite Element Model. *Traffic Injury Prevention,* **16**(Sup1): pp.S49–56.

[5] Watanabe, R., Katsuhara, T., Miyazaki, H., Kitagawa, Y., Yasuki, T. (2012) Research of the Relationship of Pedestrian Injury to Collision Speed, Car-type, Impact Location and Pedestrian Sizes using Human FE model (THUMS version 4). *Stapp Car Crash Journal,* **56**: pp.269–321.

[6] Pipkorn, B., Östh, J., *et al.* (2021) Validation of the SAFER Human Body Model Kinematics in Far-Side Impacts. *Proceedings of the IRCOBI Conference*, Online.

[7] Östh, J., Pipkorn, B., Iraeus, J., Forsberg, J. (2021) Numerical Reproducibility of Human Body Model Crash Simulations. *Proceedings of the IRCOBI Conference,* Online.

[8] Schmitt, K.-U., Niederer, P. F., *et al.* (2019) *Trauma Biomechanics: An Introduction to Injury Biomechanics*. Springer Verlag, Berlin, Germany.

[9] Östh, J., Happee, R., Brolin, K. (2012) Active Muscle Response using Feedback Control of a Finite Element Human Arm Model. *Computer Methods in Biomechanics and Biomedical Engineering,* **15**(4): pp.347–361.

[10] Östh, J., Brolin, K., Bråse, D. (2015) A Human Body Model with Active Muscles for Simulation of Pretensioned Restraints in Autonomous Braking Interventions. *Traffic Injury Prevention,* **16**(3): pp.304–313.

[11] Ólafsdóttir, J. M., Östh, J., Brolin, K. (2019) Modelling Reflex Recruitment of Neck Muscles in a Finite Element Human Body Model for Simulating Omnidirectional Head Kinematics. *Proceedings of the IRCOBI Conference*, Florence, Italy.

[12] Sugiyama, T., Kimpara, H., *et al.* (2007) Effects of Muscle Tense on Impact Responses of Lower Extremity. *Proceedings of the IRCOBI Conference*, Maastricht, the Netherlands.

[13] Iwamoto, M., Nakahira, Y., Kimpara, H., Sugiyama, T. (2009) Development of a Human FE Model with 3-D Geometry of Muscles and Lateral Impact Analysis for the Arm with Muscle Activity. *SAE Technical Paper* 2009-01-2266.

[14] Iwamoto, M., Nakahira, Y., Kimpara, H., Sugiyama, T. (2012) Development of a Human Body Finite Element Model with Multiple Muscles and their Controller for Estimating Occupant Motions and Impact Responses in Frontal Crash Situations. *Stapp Car Crash Journal,* **56**: pp.231–268

[15] Iwamoto, M., Nakahira, Y. (2015) Development and Validation of the Total HUman Model for Safety (THUMS) Version 5 Containing Multiple 1D Muscles for Estimating Occupant Motions with Muscle Activation during Side Impacts. *Stapp Car Crash Journal,* **59**: 53–90.

[16] Devane, K., Johnson, D., Gayzik, F.S. (2019) Validation of a Simplified Human Body Model in Relaxed and Braced Conditions in Low-Speed Frontal Sled Tests. *Traffic Injury Prevention,* **20**(8).

[17] Correia, M. A., McLachlin, S. D., Cronin, D. S. (2021) Vestibulocollic and Cervicocollic Muscle Reflexes in a Finite Element Neck Model During Multidirectional Impacts. *Annals of Biomedical Engineering,* **49**(7): pp.1645–1656.

[18] Prüggler, A., Huber, P., *et al.* (2011) Implementation of Reactive Human Behavior in a Numerical Human Body Model using Controlled Beam Elements as Muscle Element Substitutes. *Proceedings of the ESV Conference*, Washington, D.C.

[19] Yigit, E. (2018) *Reaktives FE-Menschenmodell im Insassenschutz*. Springer Fachmedien, Wiesbaden, Germany.

[20] Öztürk, A., Mayer, C., *et al.* (2019) A Step Towards Integrated Safety Simulation Through Pre-Crash to In-Crash Data Transfer. *Proceedings of the ESV Conference,* Eindhoven, the Netherlands.

[21] Meijer, R., Rodarius, C., Adamec, J., van Nunen, E., van Rooij, L. (2008) A First step in Computer Modelling of the Active Human Response in a Far-Side Impact. *International Journal of Crashworthiness,* **13**(6): pp.643–652.

[22] Meijer, R., van Hassel, E., *et al.* (2012) Development of a Multi-Body Human Model that Predicts Active and Passive Human Behaviour. *Proceedings of the IRCOBI Conference*, Dublin, Ireland.

[23] Kato, D., Nakahira, Y., Atsumi, N., Iwamoto, M. (2018) Development of Human-Body Model THUMS Version 6 containing Muscle Controllers and Application to Injury Analysis in Frontal Collision after Brake Deceleration. *Proceedings of the IRCOBI Conference*, Athens, Greece.

[24] Devane, K., Koya, B., Johnson, D., Gayzik, F.S. (2019) Validation of a Simplified Human Body Model for Predicting Occupant Kinematics during Autonomous Braking. *Proceedings of the Ohio State University Injury Biomechanics Symposium.*

[25] Larsson, E., Iraeus, J., *et al.* (2019) Active Human Body Model Predictions Compared to Volunteer Response in Experiments with Braking, Lane Change, and Combined Manoeuvres. *Proceedings of the IRCOBI Conference,* Florence, Italy.

[26] Brolin, K., Halldin, P., Leijonhufvud, I. (2005) The Effect of Muscle Activation on Neck Response. *Traffic Injury Prevention* **6**(1): pp.67–76.

[27] Chancey, V. C., Nightingale, R. W., van Ee, C., Knaub, K. E., Myers, B. S. (2003) Improved Estimation of Human Neck Tensile Tolerance: Reducing the Range of Reported Tolerance Using Anthropometrically Correct Muscles and Optimized Physiologic Initial Conditions. *Stapp Car Crash Journal,* **47**: pp.135–153.

[28] Behr, M., Arnoux, P.-J., Serre, T., Thollon, L., Brunet, C. (2006) Tonic Finite Element Model of the Lower Limb. *Journal of Biomechanical Engineering,* **128**: pp.223–228.

[29] Chang, C.-Y., Rupp, J. D., Kikuchi, N., Schneider, L. W. (2008) Development of a Finite Element Model to Study the Effects of Muscle Forces on Knee-Thigh-Hip Injuries in Frontal Crashes. *Stapp Car Crash Journal,* **52**: pp.475–504.

[30] Chang, C.-Y., Rupp, J. D., Reed, M., Hughes, R., Schneider, L. W. (2009) Predicting the Effects of Muscle Activation on Knee, Thigh, and Hip Injuries in Frontal Crashes Using a Finite-Element Model with Muscle Forces from Subject Testing and Musculoskeletal Modeling. *Stapp Car Crash Journal,* **53**: pp.291–328.

[31] Nie, B., Sathayanarayan, D., Ye, X., Crandall, J.R., Panzer, M.B. (2018) Active Muscle Response Contributes to Increased Injury Risk of Lower Extremity in Occupant-Knee Airbag Interaction. *Traffic Injury Prevention,* **19**: pp.S76–82.

[32] Iwamoto, M., Nakahira, Y., Sugiyama, T. (2011) Investigation of Pre-Impact Bracing Effects for Injury Outcome using an Active Human FE Model with 3D Geometry of Muscles. *Proceedings of the ESV Conference*, Washington, D.C.

[33] Alvarez, V. S., Fahlstedt, M., Halldin, P., Kleiven, S. (2013) Importance of Neck Muscle Tonus in Head Kinematics during Pedestrian Impacts. *Proceedings of the IRCOBI Conference,* Gothenburg, Sweden.

[34] Alvarez, V. S., Halldin, P., Kleiven S. (2014) The Influence of Neck Muscle Tonus and Posture on Brain Tissue Strain in Pedestrian Head Impacts. *Stapp Car Crash Journal,* **58**: pp.63–101.

[35] Iwamoto, M., Nakahira, Y. (2014) A Preliminary Study to Investigate Muscular Effects for Pedestrian Kinematics and Injuries using Active THUMS. *Proceedings of the IRCOBI Conference,* Berlin, Germany.

[36] Kato, D., Nakahira, Y., Atsumi, N., Iwamoto, M. (2018) Development of Human-Body Model THUMS Version 6 containing Muscle Controllers and Application to Injury Analysis in Frontal Collision after Brake Deceleration. *Proceedings of the IRCOBI Conferenc*e, Athens, Greece.

[37] Östh, J., Bohman, K., Jakobsson, L. (2020) Evaluation of Kinematics and Restraint Interaction when Repositioning a Driver from a Reclined to an Upright Position Prior to Frontal Impact using Active Human Body Model Simulation. *Proceedings of the IRCOBI Conference*, Munich, Germany.

[38] Gonzalez-Garcia, M., Weber, J., Peldschus, S. (2021) Potential Effect of Pre-Activated Muscles under a Far-Side Lateral Impact. *Traffic Injury Prevention,* **22**: pp.S148–152.

[39] Armstrong, R. W., Wafers, H., Stapp, J. P. (1968) Human Muscular Restraint during Sled Deceleration. *Proceedings of the 12th Stapp Car Crash Conference*, Detroit, MI.

[40] Hendler, E., O'Rourke, J., *et al.* (1974) Effect of Head and Body Position and Muscular Tensing on Response to Impact. *Proceedings of the 18th Stapp Car Crash Conference*, Ann Arbor, MI.

[41] Begeman, P. C., King, A. I., Levine, R. S. (1980) Biodynamic Response of the Musculoskeletal System to Impact Acceleration. *Proceedings of the 24th Stapp Car Crash Conference*, Troy, MI.

[42] Beeman, S. M., Kemper, A. R., Madigan, M. L., Duma, S. M. (2011) Effects of Bracing on Human Kinematics in Low-Speed Frontal Sled Tests. *Annals of Biomedical Engineering,* **39**: pp.2998–3110.

[43] Arbogast, K. B., Balasubramanian, S., *et al.* (2009) Comparison of Kinematic Responses of the Head and Spine for Children and Adults in Low-Speed Frontal Sled Tests. *Stapp Car Crash Journal,* **59**: pp.329–372.

[44] Szabo, T. J., Welcher, J. B. (1996) Human Subject Kinematics and Electromyographic Activity During Low Speed Rear Impact. *Proceedings of the 40th Stapp Car Crash Conference*, Albuquerque, NM.

[45] Magnusson, M. L., Pope, M. H., *et al.* (1999) Cervical Electromyographic Activity during Low-Speed Rear Impact. *European Spine Journal,* **8**: pp.118–125.

[46] Blouin, J.-S., Descarreaux, M., Belanger-Gravel, A., Simoneau, M., Teasdale, N. (2003) Attenuation of Human Neck Muscle Activity Following Repeated Imposed Trunk-Forward Linear Acceleration. *Experimental Brain Research,* **150**: pp.458–464.

[47] Siegmund, G. P., Sanderson, D. J., Myers, B. S., Inglis, J. T. (2003) Awareness Affects the Response of Human Subjects Exposed to a Single Whiplash-Like Perturbation *Spine,* **28**(7): pp.671–679.

[48] Östh, J., Ólafsdóttir, J. M., Davidsson, J., Brolin, K. (2013) Driver Kinematic and Muscle Responses in Braking Events with Standard and Reversible Pre-tensioned Restraints: Validation Data for Human Models. *Stapp Car Crash Journal,* **57**: pp.1–47.

[49] Yeomans, J. S., Li, L., Scott, B. W., Frankland, P. W. (2002) Tactile, Acoustic and Vestibular Systems Sum to Elicit the Startle Reflex. *Neuroscience and Biobehavioral Reviews,* **26**: pp.1–11.

[50] Snyder, R.G. (1975) *Bioengineering Study of Basic Physical Measurements Related to Susceptibility to Cervical Hyperextension-hyperflexion Injury*. University of Michigan Transport Research Institute, University of Michigan, Ann Arbor, MI.

[51] Hault-Dubrulle, A., Robache, F., Pacaux, M.-P., Morvan, H. (2011) Determination of Pre-Impact Occupant Postures and Analysis of Consequences on Injury Outcome: Part I: A Driving Simulator Study. *Accident Analysis and Prevention,* **43**: pp.66–74.

[52] Putra, I.P.A., Iraeus, J., *et al.* (2019) Comparison of Control Strategies for the Cervical Muscles of an Average Female Head-Neck Finite Element Model. *Traffic Injury Prevention,* **20**(Sup2): pp.S116–122.

[53] Winters, J. M., Stark, L. (1985) Analysis of Fundamental Human Movement Patterns Through the Use of In-Depth Antagonistic Muscle Models. *IEEE Transactions on Biomedical Engineering,* **32**(10): pp.826–839.

[54] Ghaffari, G., Brolin, K., *et al.* (2018) Passenger Kinematics in Lane Change and Lane Change with Braking Manoeuvres using Two Belt Configurations: Standard and Reversible Pre-pretensioner. *Proceedings of the IRCOBI Conference*, Athens, Greece.

[55] Leledakis, A., Östh, J., Davidsson, J., Jakobsson, L. (2021) The Influence of Car Passengers' Sitting Postures in Intersection Crashes. *Accident Analysis and Prevention,* **157**: pp. 1–13.

[56] Ghaffari, G., Brolin, K., Pipkorn, B., Jakobsson, L., Davidsson, J. (2019) Passenger Muscle Response in Lane Change and Lane Change with Braking Manoeuvres using Two Belt Configurations: Standard and Reversible Pre-pretensioner. *Traffic Injury Prevention,* **20**(S1): pp.S43–S51.

[57] Kleiven, S. (2007) Predictors for Traumatic Brain Injuries Evaluated through Accident Reconstructions. *Stapp Car Crash Journal*, **51**.

[58] Larsson, K.-J., Blennow, A., Iraeus, J., Pipkorn, B., Lubbe, N. (2021) Rib Cortical Bone Fracture Risk as a Function of Age and Rib Strain: Updated Injury Prediction using Finite Element Human Body Models. *Frontiers in Bioengineering and Biotechnology,* **9**: pp.412.

[59] Pipkorn, B., Iraeus, J., Björklund, M., Bunketorp, O., Jakobsson, L. (2019) Multi-scale Validation of a Rib Fracture Prediction Method for Human Body Models. *Proceedings of the IRCOBI Conference*, Florence, Italy.

[60] Iraeus, J., Pipkorn, B. (2019) Development and Validation of a Generic Finite Element Ribcage for Strain Based Fracture Prediction. *Proceedings of the IRCOBI Conference*, Florence, Italy.

[61] Stemper, B. D., Chivri, S, et al. (2018) Biomechanical Tolerance of Whole Lumbar Spines in Straightened Posture Subjected to Axial Acceleration. *Journal of Orthopaedic Research,* **36**(6): pp. 1747–1756.

VIII. APPENDIX

SAFER HBM Spatial Tuning Groups

The muscle activations for the SAFER HBM were calculated for eight spatial tuning groups for the cervical controller [11] (Fig. A1) and for four groups for the lumbar controller [25] (Fig. A2). All the muscles in each group, on the same side of the sagittal midplane of the body had the same activation level and resulting muscle activations in the simulation were presented and analysed in these groups.

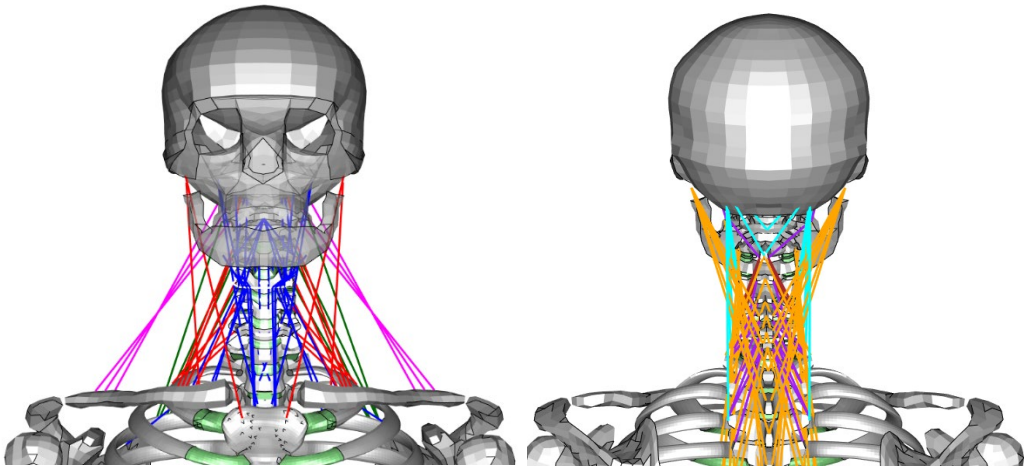

Fig. A1. Cervical muscle spatial tuning groups [11]. Red: Sternocleidomastoideus (SCM) group. Blue: Sternohyoid (STH) group. Green: Levator Scapulae (LS) group. Magenta: Trapezius (TRAP) group. Cyan: Semispinalis Capitis (SCap) group. Orange: Semispinalis Cervicis (SCerv) group. Brown: C4 level Multifidus (CM-C4) group. Purple: C6 level Multifidus (CM-C6) group.

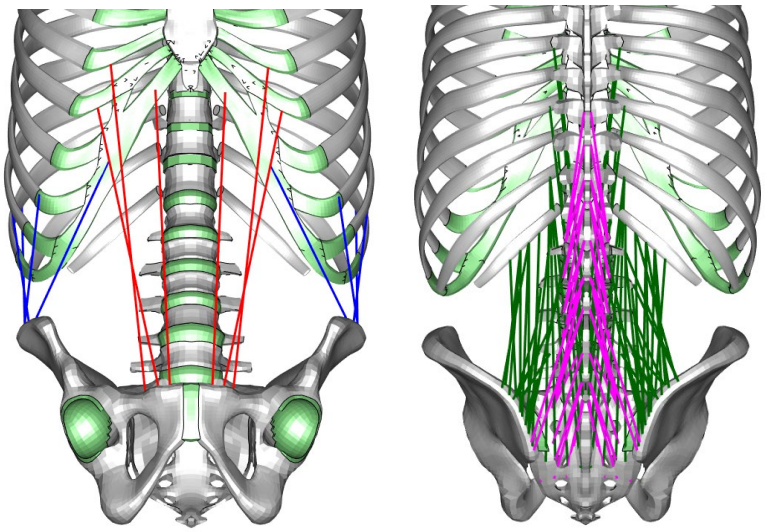

Fig. A2. Lumbar muscle spatial tuning groups [25]. Red: Rectus Abdominis (RA) group. Blue: Obliques (OBL) group. Green: Lumbar Erector Spinae (LES) group. Magenta: Lumbar Multifidus group (LMF).

Crash Controller Error Signal

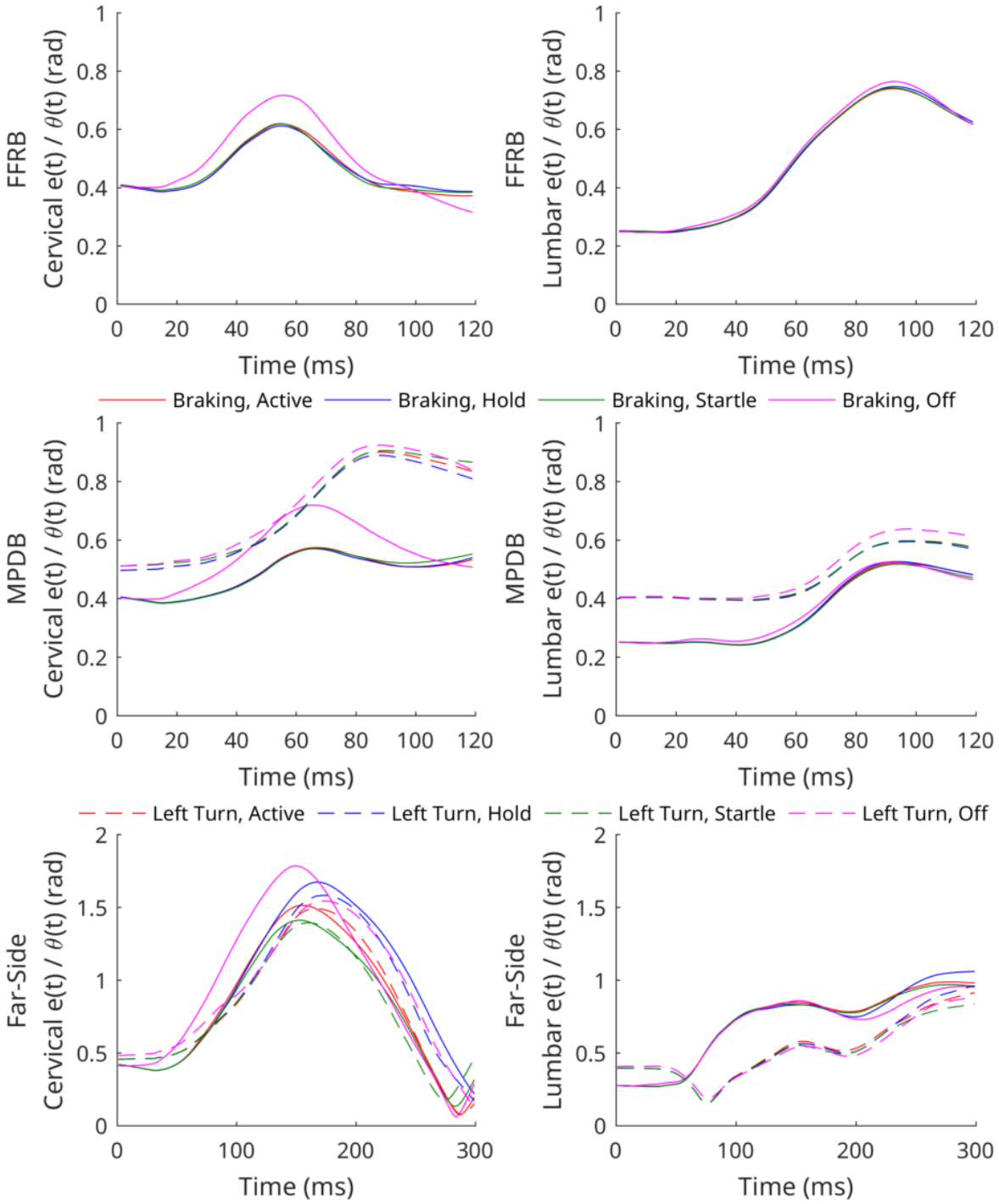

Fig. A3. Time histories of the controller error signal, *e(t)*, or *θ(t)* (Equation 1) for all crash simulations.

Crash Muscle Activations

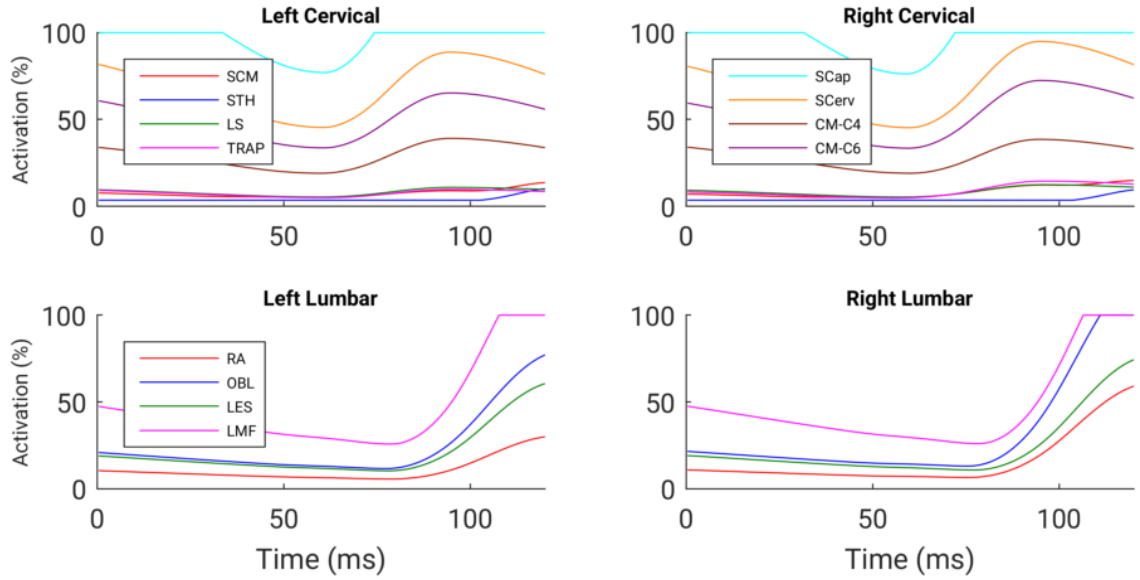

Fig. A4. Time histories of the SAFER HBM muscle tuning group activation levels during the MPDB crash after the pre-crash Braking manoeuvre with the *Active* muscle control strategy (Sequence 2).

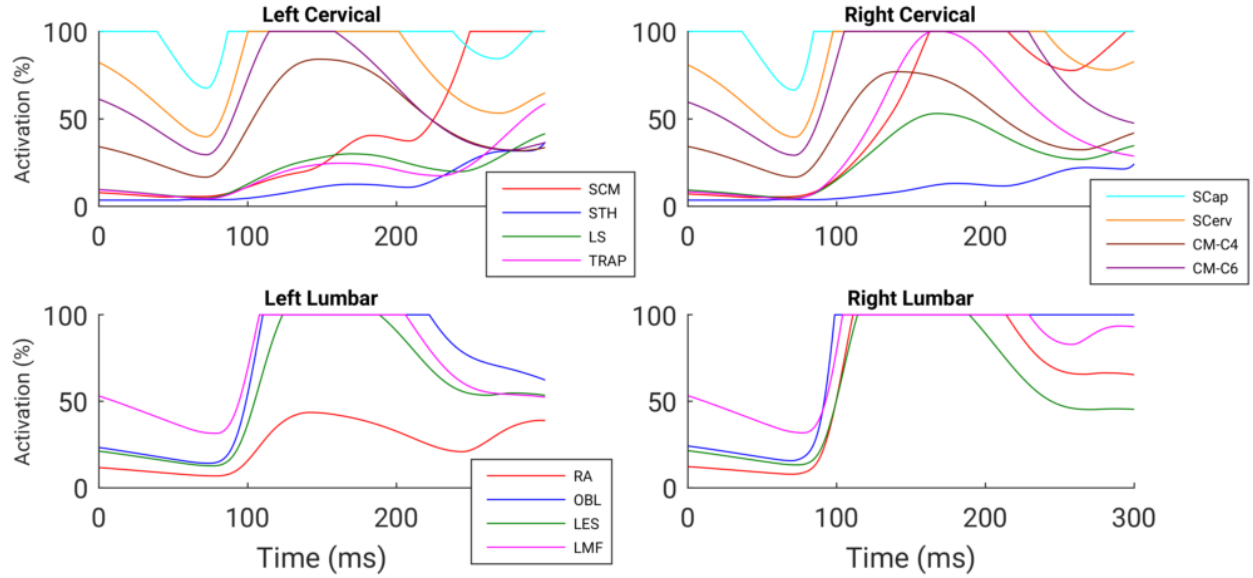

Fig. A5. Time histories of the SAFER HBM muscle tuning group activation levels during the Far-Side crash after the pre-crash Braking manoeuvre with the *Active* muscle control strategy (Sequence 3).

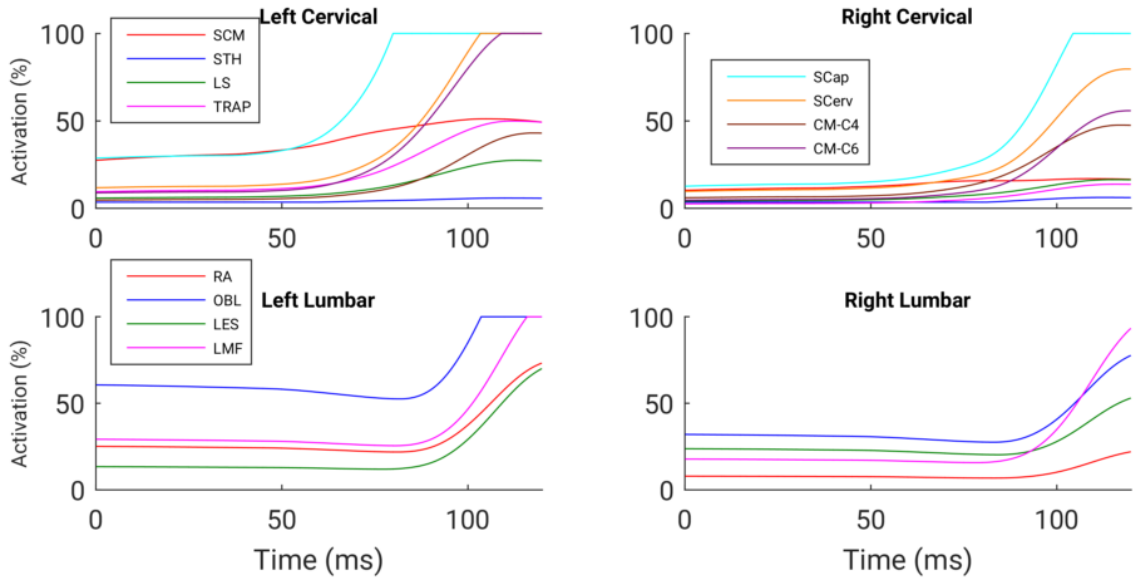

Fig. A6. Time histories of the SAFER HBM muscle tuning group activation levels during the MPDB crash after the pre-crash Left Turn manoeuvre with the *Active* muscle control strategy (Sequence 4).

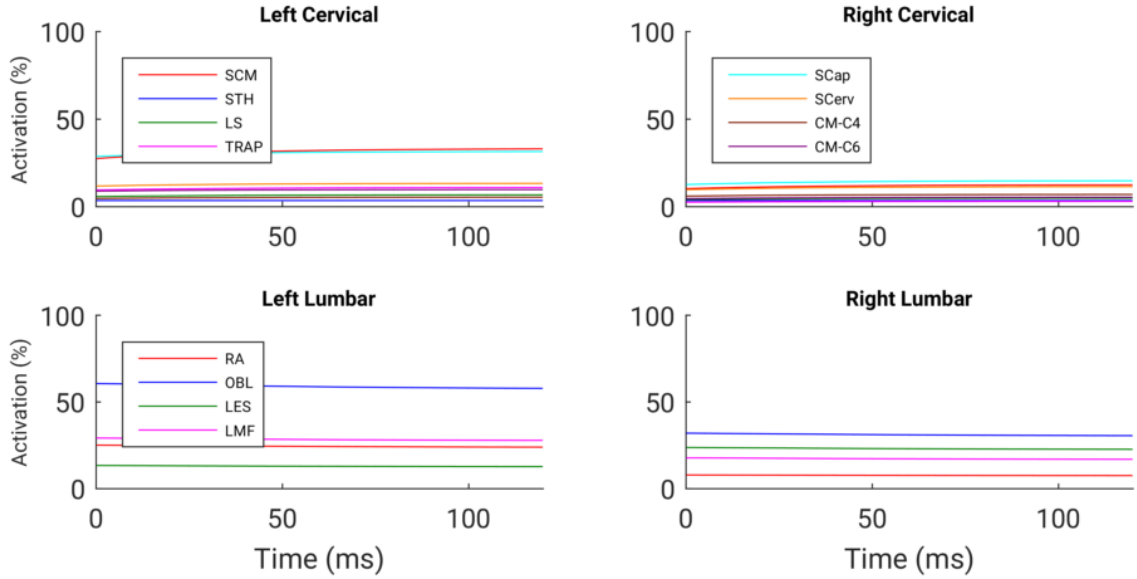

Fig. A7. Time histories of the SAFER HBM muscle tuning group activation levels during the MPDB crash after the pre-crash Left Turn manoeuvre with the Hold muscle control strategy (Sequence 4).

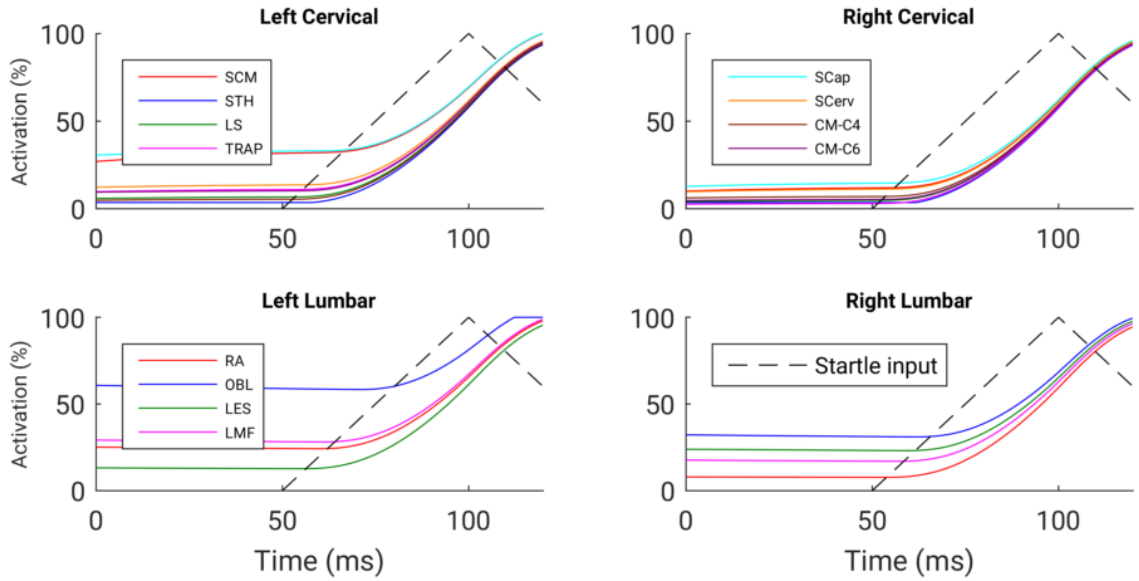

Fig. A8. Time histories of the SAFER HBM muscle tuning group activation levels during the MPDB crash after the pre-crash Left Turn manoeuvre with the *Startle* muscle control strategy (Sequence 4).

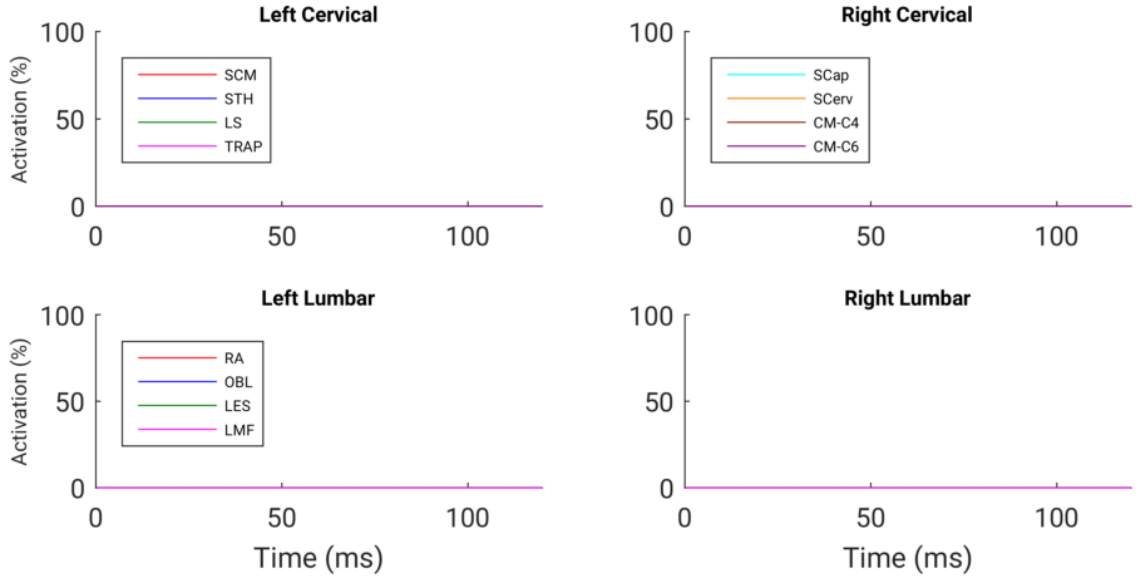

Fig. A9. Time histories of the SAFER HBM muscle tuning group activation levels during the MPDB crash after the pre-crash Left Turn manoeuvre with the *Off* muscle control strategy (Sequence 4).

Injury Prediction Time History Data

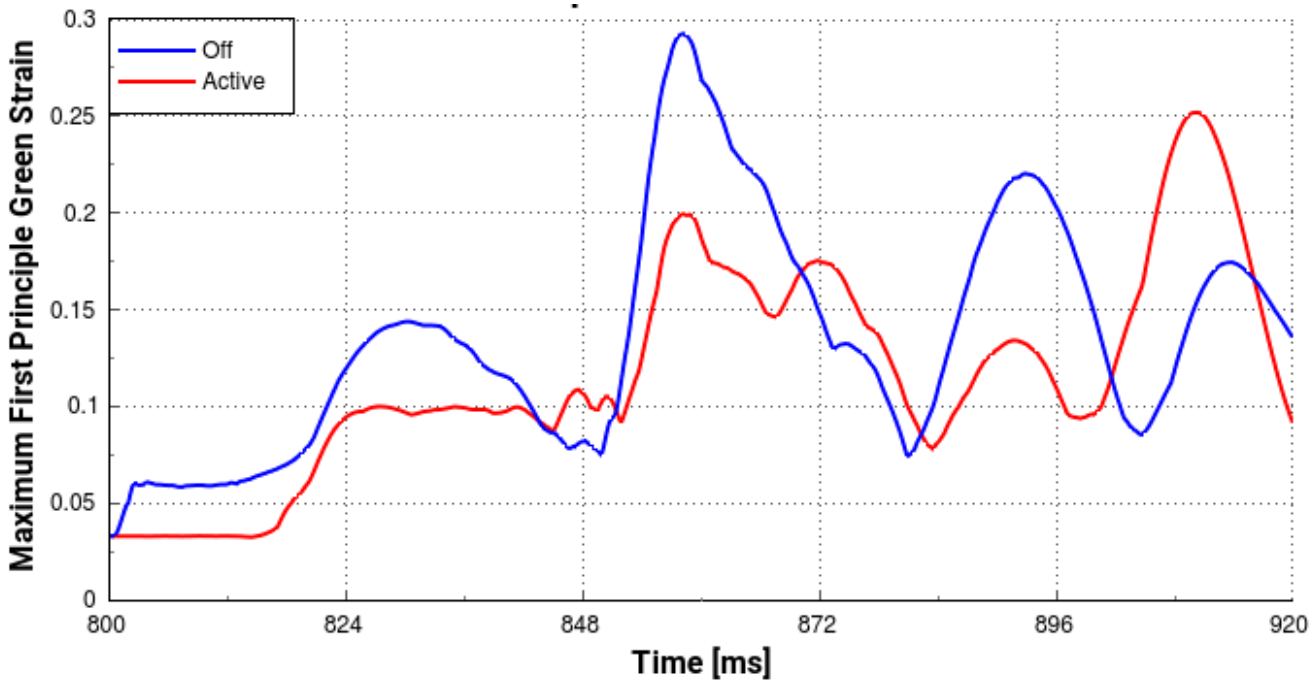

Fig. A10. Time history data for brain max principal strain for Sequence 1 (FFRB preceded by Braking) with the postural control *Active* (red) and *Off* (blue). The first 300 ms was the initialization-phase, the period 300–800 ms the Braking-phase, and the showed interval from 800–920 ms the crash-phase.

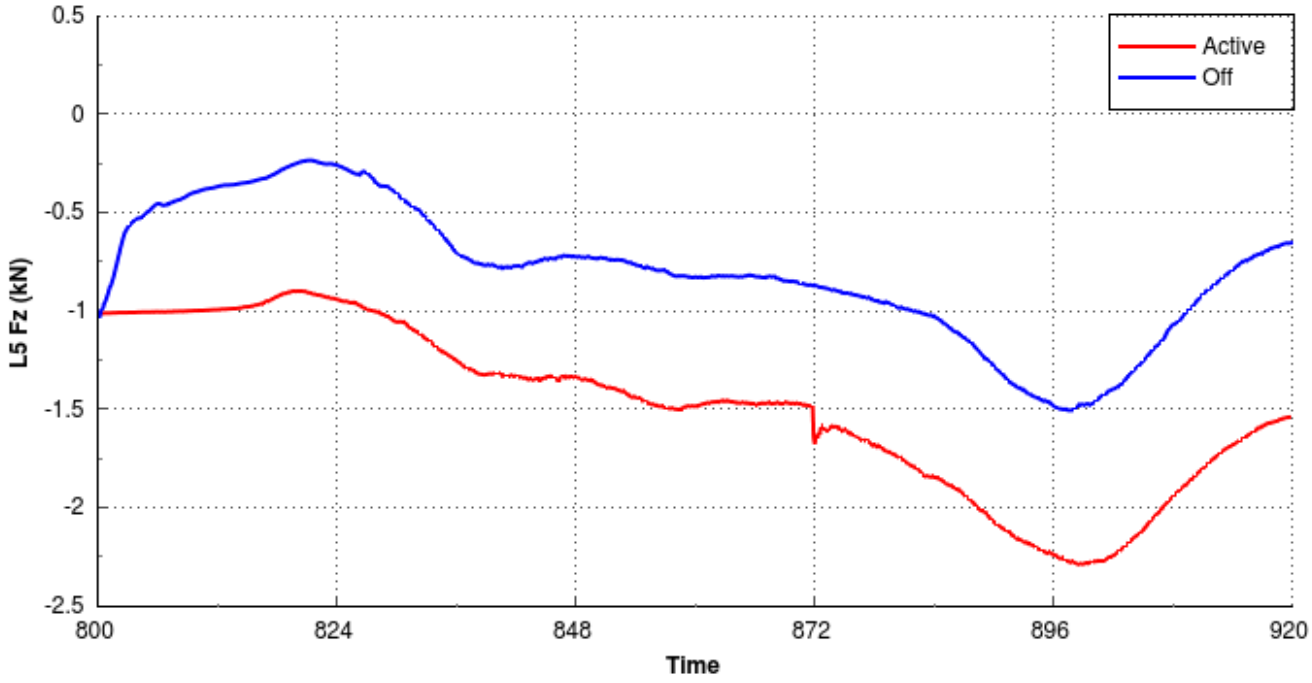

Fig. A11. Time history data for the L5 vertebra compressive Fz force in Sequence 1 (FFRB preceded by Braking) with the postural control *Active* (red) and *Off* (blue). The first 300 ms was the initialization-phase, the period 300–800 ms the Braking-phase, and the showed interval from 800–920 ms the crash-phase. For the simulation with the controller off, the muscle forces were removed at the start of the crash-phase and the compressive Fz in the lumbar spine reduced by approximately 0.8 kN.

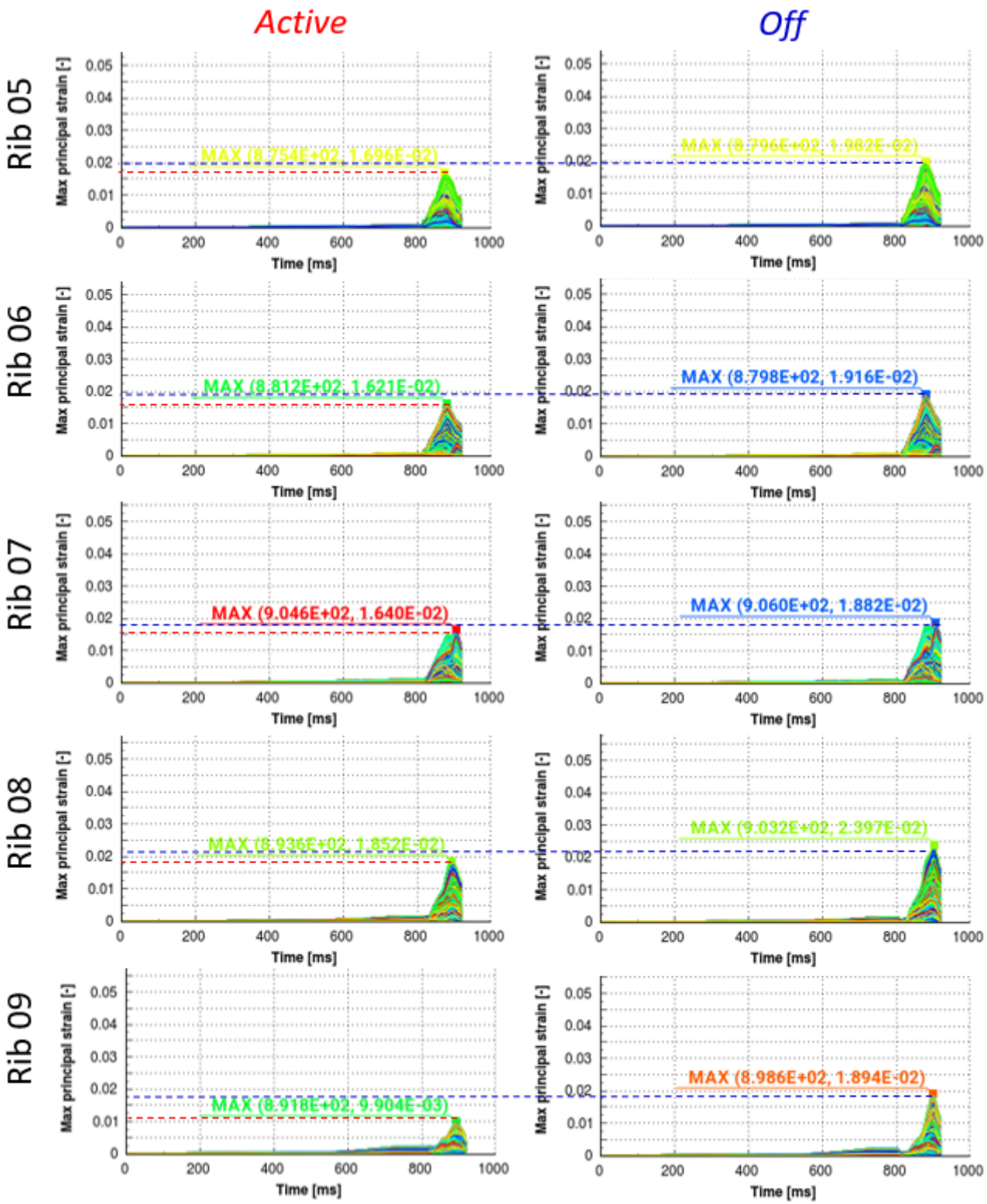

Fig. A12. Time history data for rib strain for all elements of rib 05 to rib 09 for the inboard/left side ribs for Sequence 1 (FFRB preceded by Braking) with the postural control *Active* (left) and *Off* (right). The first 300 ms was the initialization-phase, the period 300–800 ms the Braking-phase, and 800–920 ms the crash-phase. The dashed lines show the decrease in peak rib strains for the *Active* (red dashed) simulation compared with the controllers *Off* (dashed blue).